Gas-Phase Conformations of Proteolytically Derived Protein Fragments: Influence of Solvent on Peptide Conformation

Brandon T. Ruotolo and David H. Russell*

Laboratory for Biological Mass Spectrometry, Department of Chemistry, Texas A&M University, College Station, Texas 77843-3255

Received: March 3, 2004; In Final Form: July 23, 2004

The structures of 4 tryptic peptides are studied using matrix-assisted laser desorption ionization−ion mobility mass spectrometry, circular dichroism spectroscopy, and solution-phase hydrogen−deuterium exchange mass spectrometry. The sequences LLGNVLVVVLAR (bovine hemoglobin) and HGTVVLTALGGILK (horse heart myoglobin) are helical within their native proteins and as gas-phase ions [*J. Am. Chem. Soc.* **2002**, *124*, 4214]; however, the two peptides undergo very different structural transitions as their local environment is changed. For example, circular dichroism measurements suggest that the peptide LLGNVLVVVLAR assumes a β-hairpin conformation in aqueous/methanolic solvent systems; however, the helical structure of HGTVVLTALGGILK appears to be denatured (takes on a random coil conformation) upon cleavage from the protein. The gas-phase structure of the peptides exhibit a high correlation to the conformation observed by circular dichroism in 2,2,2-trifluoroethanol, suggesting that the gas-phase structure may be utilized for solution-phase relevant studies of peptide folding.

Introduction

Most current protein folding theories center around two distinct ideas that describe the onset of a folding event.[1] The "hydrophobic collapse" model assumes that the formation of protein tertiary (3°) structure is driven initially by the exclusion of water from the interior of the protein, and local secondary (2°) structure is formed following the initial "collapse".[2,3] The "hierarchical" model assumes that the formation of protein 3° structure is initiated by the formation of local 2° structure (i.e., autonomous folding subunits).[4] This model is supported by the isolation of several short peptide sequences that exhibit unusually high amounts of secondary structure under a variety of conditions (i.e., pH, solvent composition, temperature, etc.). For example, when isolated from the parent protein, the H-helix from sperm whale myoglobin and the C-peptide from ribonuclease A (residues 1−13) both retain a significant percentage of their protein-native secondary structure.[5,6] Since these initial observations, others have identified short (<20 residues) peptide sequences that take on stable secondary structure that can be related to the structure adopted by that peptide segment within the context of the corresponding native protein.[1] In addition, credence is lent to the "autonomous folding subunit" model of protein folding through the apparent success of protein folding prediction algorithms that are partly based on its principles,[7] and the recent design of miniproteins that fold into reproducible and predictable secondary/tertiary structures.[8]

Recently, mass spectrometry (MS) has emerged as a rapid means of determining the dynamics of solution-phase protein folding.[9,10] In general, mass spectrometry based protein folding techniques are attractive due to their ability to deal with complex or unpurified samples and low levels (pmoles-fmoles) of sample. For instance, Fitzgerald and co-workers have developed high-throughput methodologies for assessing monomeric protein stability,[11] multimeric protein complex stability,[12] and protein−ligand binding affinities[13] using a combination of H/D exchange MS with known methods for accessing protein denatured states (termed SUPREX). Although H/D exchange MS is useful for conceptualizing the dynamics and chemical susceptibility of protein regions, it cannot provide a residue specific picture of the protein folding event, as is possible in H/D exchange NMR experiments.[14−16]

Over the past decade, numerous mass spectrometry based methods for determining gas-phase peptide and protein structure have also evolved. For example, similar to the chemical susceptibility based methods used in solution, ion−molecule reaction chemistry has been utilized to study the structure of gas-phase proteins and peptides. The most commonly used of these techniques is gas-phase H/D exchange, in which the peptide or protein ion is allowed to react with a volatile deuterating agent (D_2O, ND_3, etc.), yielding the eventual exchange of all labile hydrogens.[17] Gas-phase H/D exchange kinetic data are convoluted by the influence of multiple factors including: the accessibility of the charge site (the site of the ion−neutral reaction), gas-phase basicity of surrounding groups, and proton bridging effects, making a detailed analysis of gas-phase exchange data difficult. Despite this apparent limitation, several groups have been able to use gas-phase H/D exchange data to obtain useful structural information on a wide variety of peptides.[18] Gas-phase ion−molecule reaction chemistry with water has also been used to investigate gas-phase ion structure of peptides and proteins. Saturation measurements have been made on both peptides and proteins, in which the number of water molecules adducted reflects a combination of the hydrophobicity and the gas-phase structure of the peptide or protein.[19] In addition, the thermodynamics of water adduction can be calculated using the relative abundances of the $[M + H]^+$ and the $[M + H + H_2O]^+$ ions, which can be related back to the gas-phase structure of the peptide or protein ion being investigated.[20]

Ion mobility spectrometry can be used to accurately measure the collision cross-section of gas-phase ions, and ion mobility

* Corresponding author. E-mail: russell@mail.chem.tamu.edu.

10.1021/jp0490296 CCC: $27.50
Published on Web 09/04/2004

data combined with molecular modeling can be used to assign structures to gas-phase ions.[21−24] For example, Jarrold and co-workers were able to distinguish misfolded versions of singly charged polyalanine-based peptides from helical and globular forms of the same peptide.[21] For larger multiply charged polyalanine ions, Clemmer and colleagues used ion mobility to distinguish α-helices ($i \rightarrow i + 4$ hydrogen bonding) from 3_{10}-helices ($i \rightarrow i + 3$ hydrogen bonding).[22] Additionally, several groups have measured collision cross-sections for protein ions over a variety of charge states and proposed Coulombically driven unfolding pathways for some protein systems.[23] Utilizing an ion trap-IM-MS method, Clemmer and co-workers showed that protein ion collision cross-sections (i.e., conformation) can change as a function of trap time, indicating the existence of metastable conformational populations for some protein ion systems.[24]

Although information applicable to the native state conformation and function is the goal of any structural study of biologically important peptides and proteins, there are significant motivations for studying proteins and peptides in non-native environments, especially in the gas phase. Studies designed to measure the influence of a single variable on a folding event are often complicated by the inability to exclude all but a single operating parameter. In the gas phase, experiments are performed on either anhydrous or partially hydrated proteins and peptides, thus simplifying both the role of solvent on observed folding events and the computational approaches designed to understand empirical folding data.[25] In another approach to ascertain the influence of solvent on peptide and protein conformation, pre-ionization solution conditions are changed in an effort to influence the resulting conformation of the gas-phase ion (i.e., "memory effects").[26] However, because data are available for only intact protein ions or protein domains, it is difficult to distinguish between the nature of specific conformational changes and the applicability of those changes to solution-phase folding events. In contrast to previous protein-based studies designed to investigate the influence of solution-phase environment on gas-phase structure, studies in our laboratory are aimed at determining specific secondary structure information for a group of peptides in both solution and gas-phase environments. Currently, our efforts are focused on the observation that certain proteolytic digest fragments have anhydrous conformations that resemble the secondary structure exhibited by the same peptides in the intact protein.[27]

This report focuses on four peptide sequences identified from peptide mass maps of bovine hemoglobin and horse heart myoglobin. Complementary conformational data obtained for these peptides using IM-MS, circular dichroism, and H/D exchange-MS are also presented. The data indicate that peptide ion secondary structure is highly dependent on environment (as expected), but a preference to form a large number of ordered intramolecular hydrogen bonds is retained upon transfer to the gas phase. In other words, the peptide ions studied here are not "denatured" but undergo structural transitions that are dependent upon solution-phase/gas-phase conditions. In addition, it is apparent from the data that peptides that are random coil (i.e., exhibit no identifiable higher-order structure) remain so throughout the MALDI sample preparation and ionization procedures. The data presented here clearly illustrate that though "memory effects" as they have been described in the literature are not observed, measurements of gas-phase structure do indeed have relevance to the solution-phase conformation of biopolymers, as IM measurements seem to correlate well with CD measurements in 2,2,2-trifluoroethanol (TFE), a solvent frequently used by biophysicists to obtain meaningful structural information for peptides and proteins. The implications of these results for both protein folding and the evaluation of solution-phase "memory effect" data are discussed.

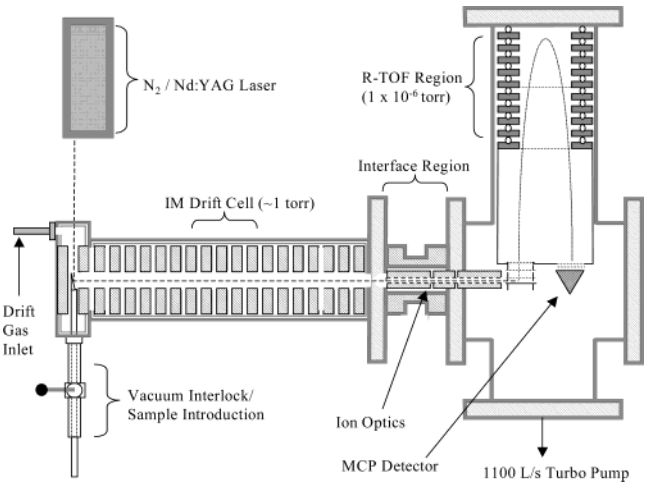

Figure 1. Schematic diagram of the MADLI−IM-TOF MS instrument used in these studies. The dashed line traces the path of ions through the instrument.

Experimental Section

Samples and Preparation. Tryptic digestion of protein samples (sequence modified, Promega, Madison, WI) was performed as described previously.[28] Briefly, hemoglobin (bovine) or myoglobin (horse heart) (Sigma, St. Louis, MO) was thermally denatured (30 min 90° C),[29] then added in a 40:1 concentration ratio with trypsin, and allowed to react for ~4 h. The resulting digested protein was mixed in a 2000:1 (matrix-to-analyte) ratio with α-cyano-4-hydroxycinnamic acid and spotted directly on the sample probe-tip. Peptide sequences LLGNVLVVVLAR (104−115 from bovine hemoglobin, β-subunit), HGTVVLTALGGILK (64−78 from horse heart myoglobin), LLVVYPWTQR (30−39 from bovine hemoglobin, β-subunit), and VEADIAGHGQEVLIR (17−31 from horse heart myoglobin) were custom synthesized (Polypeptide Laboratories GmbH, Wolfenbuettel, Germany). In addition, acetyl-HGTVVLTALGGILK (Synpep Dublin, CA) and bradykinin (RPPGFSPFR, Sigma) were purchased and used without any additional purification/preparation. All peptides were mixed with matrix (2000:1 matrix-to-analyte ratio) and laser desorbed in a manner similar to the protein digest samples.

Acetylation of the N-terminus of LLGNVLVVVLAR, LLVVYPWTQR, and VEADIAGHGQEVLIR was carried out utilizing a protocol involving treatment with acetic anhydride.[30] Briefly, peptides (10−15 μL, 100 pmol/μL) were diluted to a volume of 50 μL in a 100 mM ammonium carbonate buffer and cooled in an ice bath, and acetic anhydride was added in 5−10 μL aliquots for 1 h (until ~40−50 μL had been added). Samples were then mixed with matrix (as described above), spotted, and analyzed by both high-resolution MALDI-TOFMS (STR, Applied Biosystems, Framingham, MA) and MALDI-IM-TOFMS. In most cases, the conversion to the acetylated form of the peptide was approximately 100%.

Ion Mobility-Mass Spectrometry. The matrix-assisted laser desorption/ionization (MALDI)-IM-TOFMS used in these studies is described elsewhere.[31] As shown in Figure 1, ions are created at one end of a 30.5 cm periodic focusing drift cell using MALDI. MALDI was performed using a cartridge-type nitrogen laser (337 nm, Thermo Spectraphysics, Franklin, MA) operated

at a repetition rate of 20−30 Hz, or a frequency-tripled solid-state Nd:YAG operated at 200 Hz (355 nm, PowerChip PNV, JDS Uniphase, San Jose, CA).[32] Subsequently, the ions formed by MALDI drift through an inert gas (He, ∼1 Torr measured with a capacitance manometer (Inficon, Balzers, Liechtenstein)) under the influence of an electrostatic field (25−50 V cm^{-1} $Torr^{-1}$). After the ions elute from the drift cell they are mass analyzed by a 2-stage reflectron time-of-flight (TOF) mass spectrometer (flight times between 20 and 50 μs).[33] The details of two-dimensional drift time and TOF mass spectra acquisition have been described elsewhere.[34]

Internal Calibration of Collision Cross-Section. IM-MS trend lines are defined by fitting two-dimensional data (drift time vs *m*/*z*) to an apparent linear relationship. Over the mass range utilized in these studies (500−2000 *m*/*z*), such a fit provides a relatively high correlation coefficient (>0.98) in all cases.[35,36] Collision cross-section measurements were performed using the bradykinin $[M + H]^+$ ion (*m*/*z* 1061.2) as an internal standard.[37] A value of 245 ± 5 Å^2 was used as the reference collision cross-section for the bradykinin protonated molecule (Ω_{ref}), and the collision cross-section of the unknown (Ω_{unk}) was determined by using

$$\Omega_{unk} = [D_{unk}/D_{ref}] \times \Omega_{ref} \quad (1)$$

where D_{unk} is the measured drift time of the unknown and D_{ref} is the drift time of bradykinin $[M + H]^+$.[38] Measurements were performed at several different field strengths (ranging from 25 to 50 V cm^{-1} $Torr^{-1}$) and an average percent relative standard deviation (RSD) of <1% of the measured cross-section is obtained in all cases. Because the reference cross-section has an associated precision of ±2% RSD, all collision cross-sections reported here are ±3% RSD. This single point internal calibration provides good agreement with wide variety of published peptide collision cross-sections in the mass range of the peptides in this report.[39] The collision cross-sections determined in this manner were then compared to trial structures generated by simulated annealing.

Molecular Dynamics. Simulated annealing was performed as described previously.[27] Peptide structures were constructed using Insight II (Accelerys, San Diego, CA) and simulated annealing was performed using Cerius^2 version 4.2 (Accelerys, San Diego, CA). During the first stage of molecular dynamics, multiple starting structures were heated over the course of 280 ps in a stepwise fashion, (relaxation time = 0.1 ps, time step = 0.001 ps) starting and ending at 300 K and peaking at 1000 K utilizing the Nosé temperature thermostat (resting at a specific temperature for 10 ps every 50 K). After each annealing cycle, the peptide structure was minimized. Annealing cycles were repeated 100 times for each starting structure (generating 100 minimized structures for any given starting structure). Structures were then selected on the basis of their fit to experimental collision cross-sections and subjected to further (second stage) calculations. For second stage calculations the conditions are similar, except the structures are heated over the course of 560 ps (resting for 20 ps every 50 K) to potentially eliminate trapping the molecule in a local minimum on the potential energy surface.

Starting structures varied depending upon the sequence under investigation. For LLGNVLVVVLAR and HGTVVLTALGGILK, starting conformations included extended (ϕ = 180°, Ψ = 180°), helical (α helix, π helix, and 3_{10} helix), and β-hairpin (type I β-turn $\phi_2 = -60°$, Ψ_2 = -30°, $\phi_3 = -90°$, $\Psi_3 = 0°$; type II β-turn $\phi_2 = -60°$, $\Psi_2 = 120°$, $\phi_3 = 90°$, $\Psi_3 = 0°$) configurations in multiple positions at or near the midpoint of the sequence.[40] For LLVVYPWTQR and VEADIAGHGQEVILR, starting structures were limited to an extended form, α-helix, and a type II β-hairpin, as very little indication of defined secondary structure was observed during the course of initial calculations. The gas-phase basicity of the various amino acid residues indicates that arginine is ∼55 kJ/mol more basic than Lysine, which is ∼80 kJ/mol more basic than the N-terminus.[41] With this relative ranking of basicity, charge (i.e., the proton from the MALDI event) was placed on the C-terminal basic residue side chain in all peptide models. However, the location of charge has a strong influence on the structure of gas-phase peptide ions.[42] Therefore, all four sequences were also started from an N-terminal protonation site in multiple starting geometries (e.g., α-helix, β-hairpin, and extended). This protocol generated over 1000 trial structures each for LLGNVLVVVLAR and HGTVVLTALGGILK, and over 600 trial structures for LLVVYPWTQR and VEADIAGHGQEVILR in the first stage of dynamics, and an additional several hundred structures for each peptide in the second stage. Collision cross-sections for all peptide trial structures were calculated using an on-line version of the program developed by Jarrold.[43] In all cases the trajectory method value for the collision cross-section was taken as the calculated value.[44]

Circular Dichroism. Spectra were acquired on an Aviv 62DS model CD spectrophotometer (Aviv Associates, Lakewood, NJ). Synthetic peptides (LLGNVLVVVLAR, LLVVYPWTQR, HGTVVLTALGGILK, and VEADIAGHGQEVILR) were dissolved in 50/50 (v/v) H_2O/CH_3OH, 95/5 (v/v) H_2O/CH_3OH, or 100% 2,2,2-triflouroethanol (TFE, Aldrich, Milwaukee, WI) at a concentration of 1 mg/mL for wavelength scans (0.5 nm/ 30 s, 180−250 nm), and CD signal is reported in terms of mean residue ellipticity based on the above concentration. We recognize that because the concentration reported is not a measured value, i.e., not acquired using a standard method for the determination of peptide concentration, that the error in such a concentration can be significant, and no quantitative descriptions of the conformation(s) present under a specific set of conditions are reported. That is, the data are used to formulate a qualitative description of the dominant peptide conformation for a given solvent composition. The pH was adjusted for studies on LLGNVLVVVLAR and HGTVVLTALGGILK by adding concentrated HCL dropwise, while the pH was monitored with indicator paper. For temperature ramp experiments on LLGNVLVVVLAR, the temperature was allowed to equilibrate for several minutes before a wavelength scan was acquired.

H/D Exchange Mass Spectrometry. Solution-phase H/D exchange was performed in a sealed glovebox, operated at <3% relative humidity. Lyophilized peptides (LLGNVLVVVLAR, LLVVYPWTQR, HGTVVLTALGGILK, and VEADIAGHGQEVILR) and solid matrix (α-cyano-4-hydroxycinnamic acid) were dissolved in D_2O or CD_3OD (Aldrich, Milwaukee, WI) depending on solubility. LLGNVLVVVLAR was dissolved in a 50/50 (v/v) mix of D_2O and CD_3OD, α-cyano-4-hydroxycinnamic acid was dissolved in 100% CD_3OD, and all other peptides were dissolved in 100% D_2O. The H/D exchange reaction was allowed to proceed for ∼1 h, then matrix was added. Spotting the sample on the MALDI plate then quenched the H/D exchange reaction. Successive back-exchange reactions were performed by adding ∼5 μL of 50/50 (v/v) H_2O/CH_3OH to the sample deposited on the plate. The average time for the 50/50 H_2O/CH_3OH solution to completely evaporate was approximately 10 min. This sample redeposition technique was used 7 consecutive times to produce ∼70 min of total back-exchange. MALDI mass spectra for each 10 min interval were acquired on a high-resolution MALDI-TOFMS (Voyager DE

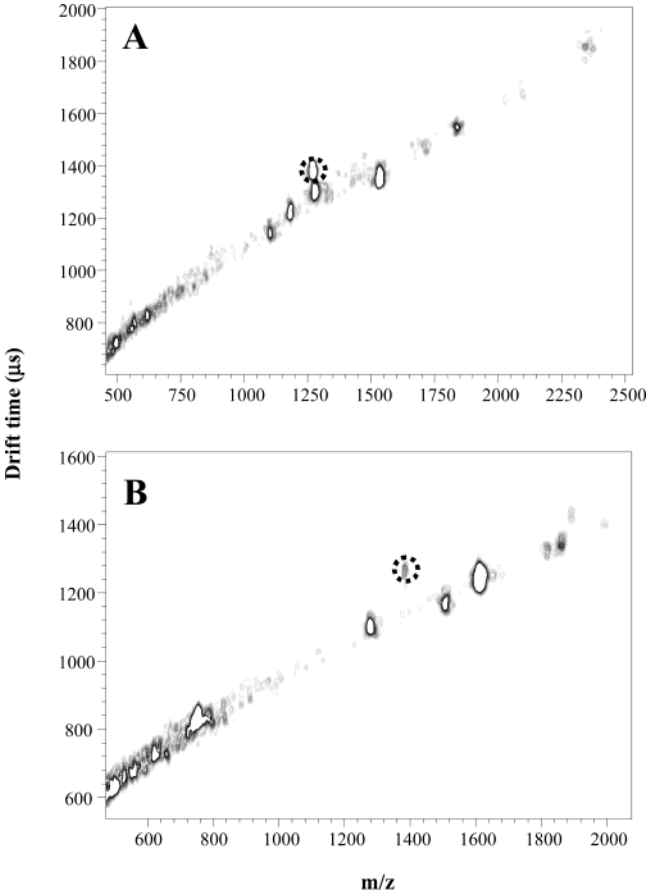

Figure 2. (A) Drift time vs *m*/*z* plot for a tryptic digest of bovine hemoglobin, where the circled ion signal corresponds to the sequence LLGNVLVVVLAR (H_O). (B) Drift time vs *m*/*z* plot for a tryptic digest of horse heart myoglobin, where the circled ion signal corresponds to the sequence HGTVVLTALGGILK (M_O).

STR, Applied Biosystems, Framingham, MA) in the reflected, positive ion mode. To mitigate the effects run-to-run variations in parameters such as pH, temperature, and exchange time on the results presented, H/D exchange experiments performed on the sequences LLGNVLVVVLAR and HGTVVLTALGGILK were conducted in the presence of several different controls (i.e., in the context of peptide mixtures in addition to experiments on the isolated peptides) including the respective control peptides (LLVVYPWTQR and VEADIAGHGQEVILR), all four peptides focused on in the manuscript, and within the context of the complete compliment of all protein digest fragments for each, the hemoglobin and myoglobin peptides. In all cases, the relative difference in exchange rates reported as significant were identical.

Results

The initial observation that some gas-phase tryptic peptides have elongated (noncompact) secondary structure was made from the two-dimensional drift time−*m*/*z* plots shown in Figure 2. The ion signals indicated by dashed circles (sequence LLGNVLVVVLAR in Figure 2A and sequence HGTVVLTALGGILK in Figure 2B) exhibit 10% relative deviations to a linear fit. From additional experiments we have found that roughly 3% of tryptic peptide sequences exhibit deviations of this magnitude.[35] Although an oversimplification of the complex relationship between ion drift time and ion *m*/*z*, this linear approximation is potentially useful for rapidly identifying peptides that are "outliers" relative to a large peptide population.

TABLE 1: Collision Cross-Section Comparison of Acetylated/Nonacetylated, Sodiated, and Protonated Peptides[a]

sequence	$[M + H]^+$ (Å^2)	$[M + Na]^+$ (Å^2)	$[Ac - M + H]^+$ (Å^2)
LLGNVLVVVLAR (H_O)	295 ± 3	286 ± 3	300 ± 3
LLVVYPWTQR (H_C)	281 ± 3	279 ± 3	283 ± 3
HGTVVLTALGGILK (M_O)	326 ± 3	315 ± 3	333 ± 3
VEADIAGHGQEVLIR (M_C)	323 ± 3	323 ± 3	326 ± 3

[a] All collision cross-sections measurements are reported relative to $[M + H]^+$ Bradykinin (245 ± 5 Å^2).

One of the goals of this study is to investigate the validity and utility of trend line analysis for the rapid determination of peptide secondary structure. To simplify the presentation of these data, the following conventions are used to refer to the tryptic peptides investigated in this report: LLGNVLVVVLAR as hemoglobin peptide-outlier (H_O), LLVVYPWTQR as hemoglobin peptide-trend line correlated (H_C), HGTVVLTALGGILK as myoglobin peptide-outlier (M_O), and VEADIAGHGQEVILR as myoglobin peptide-trend line correlated (M_C), respectively.

Ion Mobility-Mass Spectrometry and Molecular Dynamics. Initial electrospray ionization (ESI) IM-MS studies on the mobility of gas-phase tryptic peptide ions indicated that the most probable conformation for the majority of sequences was a close-packed, charge-stabilized structure (i.e., no α-helices, β-hairpins, etc.). The ion collision cross-section then depends exclusively on the packing efficiencies of the various amino acids in the sequence.[36] Using appropriate scaling factors, cross-section contributions for each amino acid, termed intrinsic size parameters (ISP), can be used to obtain good agreement with experimental collision cross-sections. Shvartsburg and co-workers utilized scaled ISP values derived from the atomic radii of the constituent atoms present in a given amino acid and demonstrated a high degree of correlation between these empirically derived ISPs and those derived from ESI-IM-MS data.[45] These empirically derived ISP values were used to determine if the differences in drift time observed in Figure 2 could be attributed to different amino acid sequence packing efficiencies. Utilizing the atomic radii that would provide the greatest variation among cross-section predictions, H_O is predicted to be approximately 1% larger than H_C (in comparison with the >5% measured by experiment), and M_C is predicted to be 8% larger than M_O, whereas measured collision cross-sections are nearly identical (within 1%).[46] Collision cross-section measurements for the four protonated peptides are listed in Table 1 (column 2). As noted, tryptic peptides from bovine hemoglobin are separated by a >5% difference in collision cross-section, whereas the tryptic peptides from horse heart myoglobin have nearly identical (differing by <1%) collision cross-sections. Clemmer and co-workers reported a value of 283 Å^2 for H_O using ESI-IM-MS, which agrees well with that obtained in these studies (281 Å^2).[36]

To determine the possible structural motifs that could give rise to the observed difference in collision cross-section, several stages of molecular dynamics simulations were performed. During the course of these dynamics simulations significant clusters (irrespective of MD energy) for both helical and β-hairpin type structures were observed for M_O and H_O, whereas the sequences H_C and M_C exhibited little evidence of recognizable biologically relevant secondary structures. The collision cross-sections of helical and β-hairpin conformational populations for M_O and H_O exhibit a high degree of overlap; i.e., these two conformational types would be nearly indistinguishable on the basis of conventional ion mobility separation alone. For

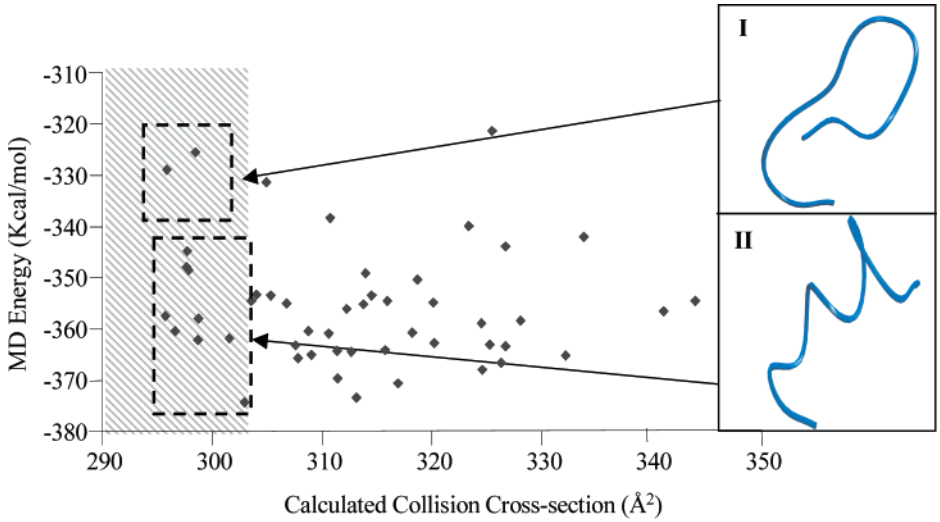

Figure 3. Scatter plot of MD energy vs calculated collision cross-section for a 560 simulated annealing run for the sequence LLGNVLVVVLAR (H_O) started from a helical structure found in the first stage of simulated annealing. The crosshatched region from ~290 Å^2 to 304 Å^2 indicates the range of the measured collision cross-section. The two areas indicated by dashed-boxes, as well as the conformations (insets **I** and **II**), are discussed in the text.

example, simulated annealing results for H_O yield a helical structure with a calculated 0.007% difference in collision cross-section. To distinguish between two such structures would require a mobility resolution of approximately 215, which is beyond the capabilities of the current instrumentation (typical resolution $\sim 30-50$).[47]

Figure 3 contains an example scatter plot of calculated MD energy vs calculated collision cross-section for H_O. Two structures from molecular dynamics simulations are shown to highlight the apparent stability differences between gas-phase β-hairpin and α-helical conformations for these sequences. Figure 3 contains data for the first 50 structures from second stage simulated annealing (560 ps duration) on the sequence H_O, protonated on the C-terminal arginine side chain. Two general energy plateaus are observed (indicated by dashed boxes), where the first plateau is composed completely of helical geometries (represented by conformer II), and the second is composed primarily of β-hairpin type structures (represented by conformer I) as well as a small number of random coil or partially helical structures. The crosshatched region of the plot corresponds to the range of collision cross-sections observed experimentally.

Simulations performed in our laboratory, and by others, indicate that the placement of ionic charge is crucial for gas-phase secondary structure formation.[42,49] To evaluate the influence of charge placement on the gas-phase structure, the collision cross-sections of N-terminally acetylated forms of the four tryptic peptides were measured and are reported in Table 1 (column 4). Parts A and C of Figure 4 show plots of drift time versus *m*/*z* that illustrate the observed relationship between the protonated peptide and the acetylated protonated peptide. N-terminal acetylation of H_O (Figure 4A) increases the observed drift time of the peptide, and therefore the collision cross-section, whereas the sequence H_C (Figure 4C) exhibits little difference in drift time between acetylated and nonacetylated analogues. Apparent differences in the drift time profile observed in Figures 4 and 5 are due to disparity in signal-to-noise between $[M + H]^+$ and $[Ac - M + H]^+$ signals.

Cross-section measurements for $[M + Na]^+$ ions of all four tryptic peptides are listed in Table 1 (column 3). Plots of drift time versus *m*/*z* illustrating differences observed between $[M + Na]^+$ and $[M + H]^+$ ion signals for H_O and H_C are shown in Figure 4B,D. A decrease in drift time is observed for the $[M + Na]^+$ ion signal for H_O relative to $[M + H]^+$; however, no such decrease is observed for H_C. The observation of a smaller collision cross-section for $[M + Na]^+$ relative to $[M + H]^+$ is consistent with the ISP analysis in this study in that the difference between the collision cross-sections for the $[M + Na]^+$ of H_O and H_C is within the error of the predicted difference. Similar results were obtained for M_C and M_O, although the differences between the cross-sections for the $[M + Na]^+$ ions did not exhibit good agreement with the ISP predicted value (difference of 5%).

Representative low-energy structures from the simulated annealing experiments are shown in Figure 5, for H_O (helical, Figure 5A), H_C (random coil, Figure 5B), M_O (helical, Figure 5C), and M_C (random coil, Figure 5D). Additional data were acquired in regard to solution-phase/gas-phase conformational memory effects including MALDI-IM-MS data for a tryptic digest of bovine hemoglobin dissolved in a 50:50 TFE/methanol solution (data not shown). No change in the positions of the peptides was observed by changing the solvent composition.

Circular Dichroism. The secondary structure of all four peptides in three different solution environments, 50:50 methanol/water, 5:95 methanol/water, and TFE (the first of which is intended to mimic the solution conditions used for the MALDI-IM-TOFMS experiment shown in Figure 2) was investigated by CD (Figure 6). Key spectral features present in the spectra shown in Figure 6 necessary to infer information concerning peptide conformation include: α-helical (minima at 222 and 208 nm, seen in Figure 6A,C,D) β-hairpin (single minimum at 220 nm, seen in Figure 6A,C), and random coil (single sloping minimum at <200 nm, seen in Figure 6B−D) spectral fingerprints. In addition to the spectra shown in Figure 6, CD spectra were taken for H_O and M_O at elevated temperatures (up to 90 °C) utilizing water as a solvent (data not shown). The peptide H_O exhibited considerable conformational integrity as a function of temperature (CD spectrum has similar features to that shown for 5/95 methanol/water in Figure 6); however, the absolute intensity of the observed signal decreased indicating some unfolding.

To further investigate the effect of pH on the structure of the peptides used in this study, CD spectra were acquired for M_O and H_O in 50:50 methanol/water at a pH of 2 (shown in Figure

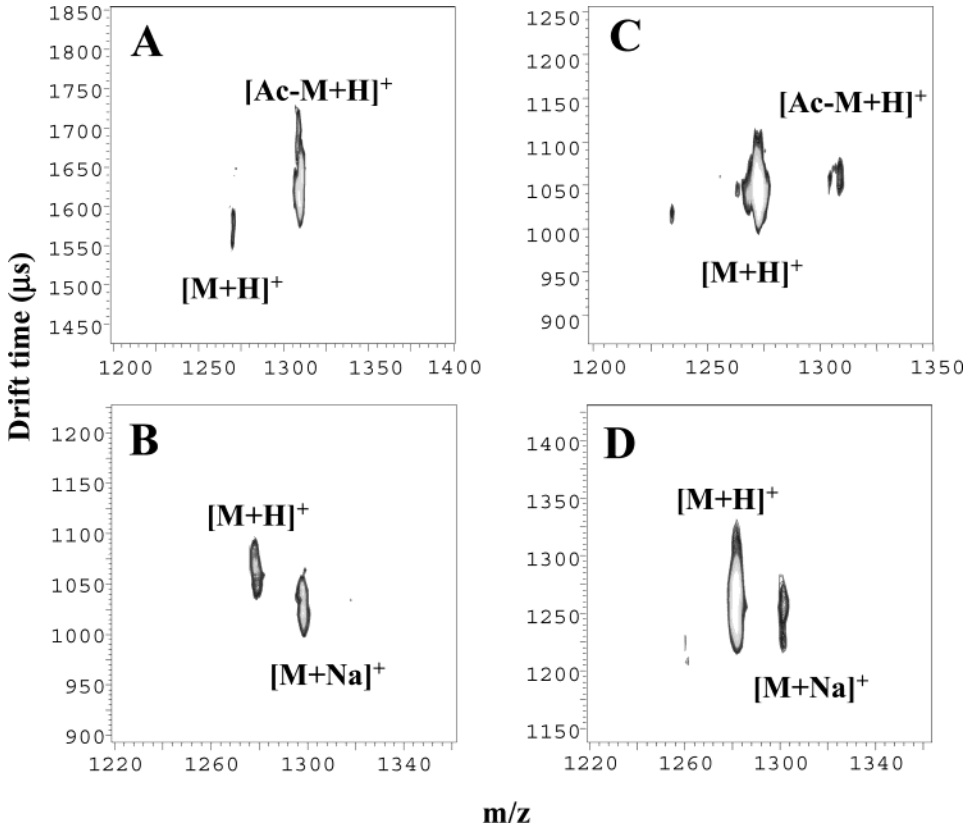

Figure 4. Drift time vs *m/z* plot illustrating the differences observed for the sequence LLGNVLVVVLAR (H_O) for (A) $[M + H]^+$ and $[Ac - M + H]^+$ (28 V cm^{-1} Torr^{-1}) and (B) $[M + H]^+$ and $[M + Na]^+$ (43 V cm^{-1} Torr^{-1}). Similar data are shown for the sequence LLVVYPWTQR (H_C) for (C) $[M + H]^+$ and $[Ac - M + H]^+$ (40 V cm^{-1} Torr^{-1}) and (D) $[M + H]^+$ and $[M + Na]^+$ (35 V cm^{-1} Torr^{-1}).

8). The CD spectrum for M_O displays a sharp minimum at ~190 nm, indicative of a random coil type conformation, whereas the CD spectrum for H_O retains β-hairpin character (as indicated by the strong minimum at 220 nm). The low-pH CD data, in combination with the H/D exchange data, suggest that the conformation of only one peptide (H_O) is retained upon the addition of matrix to the peptide solution.

H/D Exchange Mass Spectrometry. To probe the effect of matrix on peptide conformation, we carried out solution-phase H/D exchange mass spectrometry utilizing a back-exchange strategy based on several peptide resolvation steps directly from a MALDI dried droplet. These measurements were carried out on a MALDI-high resolution TOF instrument (see Experimental Section). As illustrated in Figure 7, peptides undergo nearly complete exchange in the initial period (~1 h), and each back-exchange step exposes the peptide to protonated solvent for an estimated 10 min. Inspection of Figure 7, which shows the H/D exchange mass spectra for H_O and H_C under three H/D exchange conditions (no back-exchange, 10 min of back-exchange, and 70 min of back-exchange), reveal differences in the availability of labile hydrogens between the two peptides. H_O exhibits both a broader distribution of initial exchanges (Figure 7A, II $- t =$ 0 min), a broader range of initial back-exchange (Figure 7A, III $- t =$ 10 min), and an apparently bimodal distribution of exchangeable hydrogens at long back-exchange times (Figure 7A, IV $- t =$ 70 min) when compared with H_C (Figure 7B). It is important to note that control experiments were performed to ensure that the peptides were undergoing the same exchange time by performing H/D exchange on both mixtures of the two synthesized peptides and on a sample of digested protein (see Experimental Section). Similar H/D exchange MS experiments were performed on the M_O and M_C, the results from which are shown in Figure 7C,D. Although some broadening of the isotopic profile is observed for M_O on the first step of back-exchange, similar isotope clusters are observed for both peptides upon initial H/D exchange and on complete back-exchange, indicating that both peptides are denatured (random coil) under these conditions.

Discussion

The stability and formation of biomolecular conformation is primarily described in terms of a balance of a few key forces, including (in no particular order of importance): hydrogen bonding, packing interactions, and hydrophobic forces. Gas-phase experiments introduce an additional force that is important for the formation of secondary structure, i.e., the stabilization of ionic charge, but it is not necessarily clear how the influences of the other three forces are affected when the molecule is transported to the gas phase.[48] Pioneering work by Jarrold suggests that a helical conformation can both stabilize ionic charge and an extended conformation through favorable interactions of the ionic charge at the C-terminus of a peptide with the macrodipole of the helix, indicating that some of the forces that dominate biomolecular conformation in aqueous environments (i.e., hydrogen bonds) are conserved in the gas phase.[49] Work presented here suggests that even more of the rules that dictate solution-phase folding may also apply in the gas phase, as illustrated by the high correlation between gas-phase peptide ion conformation and the conformation of peptides solvated in TFE. In effect, this work supports the notion that the gas phase should be viewed as an environment that represents an extreme on the hydrophobicity/dielectric constant scale, rather than an environment that is completely alien to chemical biology.

MALDI versus ESI for Investigations of Gas-Phase Conformation. Recent experiments in gas-phase peptide folding

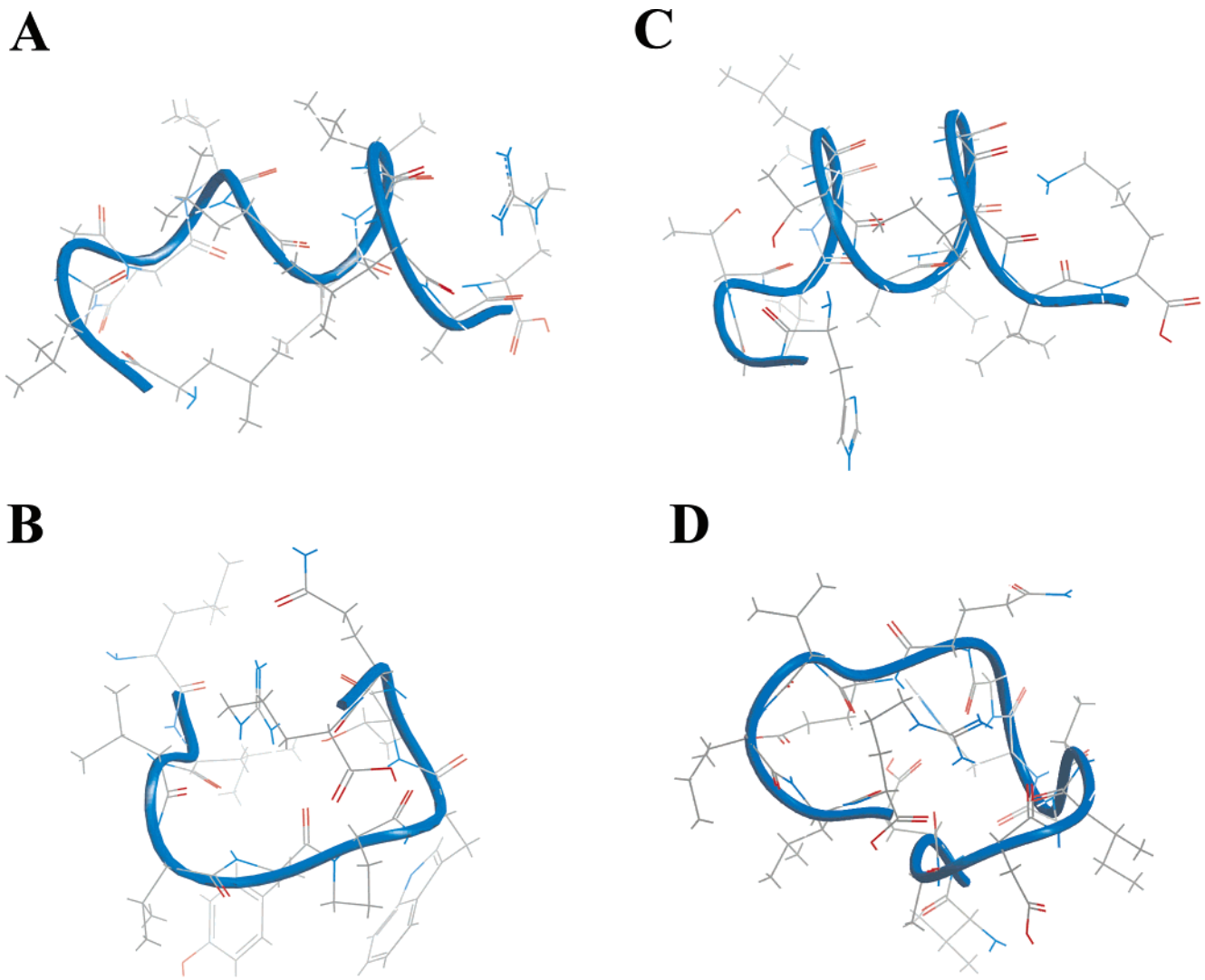

Figure 5. Structural assignments for the $[M + H]^+$ ions (A) LLGNVLVVVLAR (H_O), (B) LLVVYPWTQR (H_C), (C) HGTVVLTALGGILK (M_O), and (D) VEADIAGHGQEVILR (M_C).

have also been dominated by electrospray ionization, where MALDI has been utilized less frequently. Although there is a substantial amount of literature, including reports of X-ray crystal structures, that supports the notion that solution-phase conformation can be trapped within a crystalline state,[50] it is reasonable to assume that the final gas-phase conformation of a molecule is based primarily on intramolecular interactions and ionic charge stabilization rather than its method of formation. Generally, the data presented here support MALDI as an ionization method for the study of gas-phase conformation as it relates to solution-phase structure, as each environment (i.e., MALDI sample solution, MALDI sample deposit, TFE solution, gas phase) must be viewed independently for molecules of the size and flexibility studied here.

Assignment of Gas-Phase Conformation. Clearly, the ISP analysis indicates that the observed differences in collision cross-section are not strictly related to packing efficiency differences, and the MD results, as shown in Figure 3, favor a helical structure over a β-hairpin type structure. Such data form part of the rationale for our assignment of a helical gas-phase conformation to H_O and M_O rather than β-hairpin. Although MD energy cannot be used as a quantitative measure of the stability of these conformations, qualitatively, the helical structure is more energetically favorable of the two structures.[51] In addition, out of the 11 structures of the 50 shown that agree with the measured collision cross-section, 9 are helical and 2 are β-hairpin type structures, providing further evidence as to the relative stability of the two conformer types (helix and hairpin) for H_O in the gas phase.

The simulated annealing results (Figure 3) are similar to those described by Jarrold and co-workers. For example, they reported that β-hairpin type conformations are not as favorable as helical geometries for a series of polyvaline-based peptides on the basis of ion mobility measurements in combination with MD simulations.[52] Further evidence is provided by the preponderance of reports that identify sequences that adopt helical structures in the gas phase compared to the relatively few reports of gas-phase β-hairpins.[49,53] This low observation frequency can be rationalized in terms of the forces that are known to stabilize peptide structure in the gas phase. Although β-hairpin structures share an equivalent ability to form intramolecular hydrogen bonds, they lack the ability to solvate an ionic charge located on the C-terminal side chain as effectively as it is stabilized in helical structures (i.e., through interaction with the macro-dipole of the helix).[52]

To test the validity of the molecular dynamics results, several modified versions of the four peptides were investigated using IM-MS. The N-terminus of the peptides was acetylated to further test the helical propensity of the tryptic peptides. As indicated by the values listed in Table 1 (column 4), an increase in

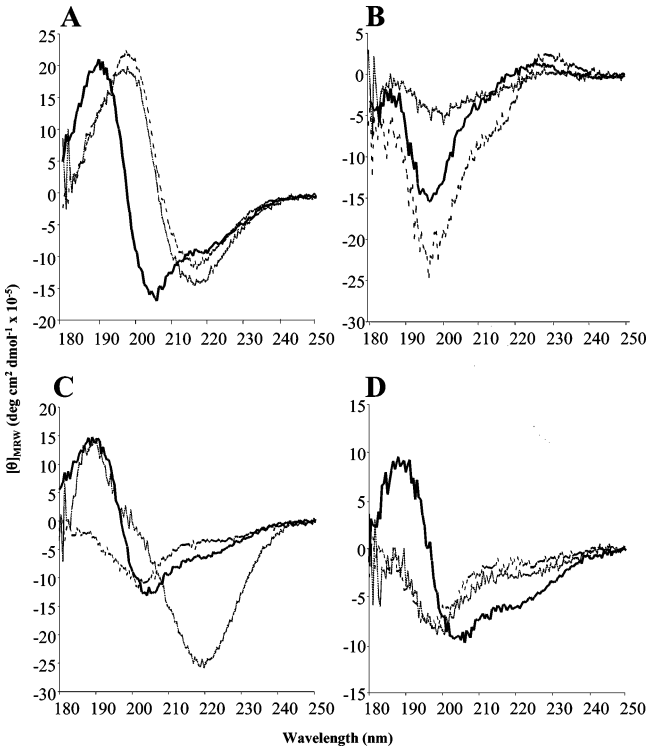

Figure 6. CD spectra of (A) LLGNVLVVVLAR (H_O), (B) LLVVYPWTQR (H_C), (C) HGTVVLTALGGILK (M_O), and (D) VEADIAGHGQEVILR (M_C) for three different solvent systems: 50:50 methanol/water (gray solid line), 5:95 methanol/water (black dashed line), and TFE (solid black line) at a pH of ~5.

collision cross-section is observed for the acetylated tryptic "outlier" peptides (M_O and H_O) and static behavior with regard to cross-section for the acetylated peptides that lie on the peptide trend (M_C and H_C). Protecting the N-terminus of a peptide is known to increase the helicity of the peptide in both the solution and gas phases, presumably by localizing the charge on the helix-favorable C-terminal position.[42,49] In addition, there is no evidence that such a modification either stabilizes β-hairpin structure or has been shown to cause a β-hairpin−helix transition. Therefore, the increase in collision cross-section observed in the acetylation experiments for these peptides is consistent with an assignment of some helical propensity for H_O and M_O, and a lack of helical propensity for H_C and M_C in the gas phase.

In addition, the collision cross-section of $[M + Na]^+$ ions (rather than $[M + H]^+$ ions) were measured to test whether the position of ionic charge had the expected, denaturing influence on the gas-phase helical peptides, as indicated by a decrease in the $[M + Na]^+$ ion collision cross-section relative to the $[M + H]^+$. The measurement of $[M + Na]^+$ ions further tests the conformational assignments from MD simulations for H_C and M_C as random coil in the gas phase as well.[38] It is important to note that alkali adduction has also been observed to increase helicity in some sequences, but only in cases where side-chain interactions have little influence on gas-phase structure.[54] As mentioned previously, good agreement between the ISP analysis and the measurements of $[M + Na]^+$ were achieved for the hemoglobin peptides, but similar agreement was not observed for M_C and M_O (difference of 5% by measurement of Na-bound ions, whereas ISP predicts a difference of 8%). This discrepancy could indicate that Na^+ adduction completely denatures the gas-phase structure of H_O (e.g., binding with carbonyl oxygens on the backbone of the molecule) but complete denaturation is not observed for M_O. The influence of alkali adduction on peptide structure is the subject of ongoing studies in our laboratory.[55]

The data presented in Figures 3 and 4, in conjunction with the ISP analysis, are consistent with a helical structure assignment for the gas-phase $[M + H]^+$ ions of H_O and M_O. Figure 5 shows representative structures from simulated annealing that correlate with the measured collision cross-sections (within 3% RSD) and are consistent with the discussion above. Figure 5A shows a helical structure that illustrates the structural motifs observed in the MD simulations of low-energy H_O helices. As observed by Jarrold and co-workers for model α-helices, the charge carrying C-terminal residue wraps around to interact with the carbonyls on the peptide backbone (the charge site in Figure 5A is 2−3 Å away from 4 backbone carbonyls), which are oriented with respect to the helix macro-dipole. In addition, the N-terminus of the structure shown in Figure 5A is unfolded and turns in toward the C-terminus, giving the peptide a more compact shape. Figure 5B illustrates a typical, compact, low-energy structure, which is favored for trial structures that match the measured collision cross-section of H_C. The C-terminal charge site is turned toward the N-terminus and is within 2−3 Å of 3−4 carbonyl oxygens. Similar structures for M_O and M_C are shown in Figure 5C,D, respectively. Again, Figure 5C illustrates the stabilization of the charge on the C-terminal side chain through interaction with macrodipole aligned carbonyls on the backbone of the peptide. In this case, the charge site is within 2−3Å of 5 different carbonyl sites. The ionic charge for the structure of M_O in Figure 5D is stabilized through interactions with both the C-terminus and multiple backbone/side-chain carbonyls.

Assignment of Solution-Phase Conformation. CD data indicate that H_C and H_O (from bovine hemoglobin) exhibit conformational trends similar to those observed for their gas-phase ion analogues, as shown in Figure 6A,B. For example, the peptide H_C exhibits random coil type behavior in all three solution compositions, as indicated by the strong minima at 190 nm. On the other hand, the CD spectra for H_O suggests that the peptide assumes β-hairpin structure in both 50:50 methanol/water and 5:95 methanol/water solutions (minima at 220 nm), and helical structure in TFE (indicated by the double minima at 207 nm and 222 nm). The observed difference in conformation between methanolic and TFE solutions are interpreted to corroborate the gas-phase structural assignment for H_O. Although both methanol and TFE act to promote intramolecular hydrogen bonding within the peptide by promoting intramolecular hydrogen bonding and increasing the influence of ionic charge,[56] the use of TFE as a solvent has been shown to be more effective at this process, because TFE exhibits a poorer hydrogen bond acceptor site and a lower dielectric constant than methanol.[57] Thus, the TFE solvent environment, where intramolecular hydrogen bonding is most favorable and the dielectric constant is at its lowest, more closely resembles a gas-phase environment out of the three solvent compositions utilized in this study and, by extension, supports the assignment of a helical conformation to the gas-phase H_O protonated ion and the assignment of random coil character to the H_C ion.

The above discussion applies to interpreting the influence of inter/intramolecular hydrogen bonding on peptides in solution and gas-phase environments, but the ideas do not take into account the importance of ionic charge stabilization on the gas-phase peptide structure.

Close inspection of the CD data for M_O and M_U shown in Figure 6C,D indicates a more complex conformational dependence on solution composition than observed for H_O and H_C.

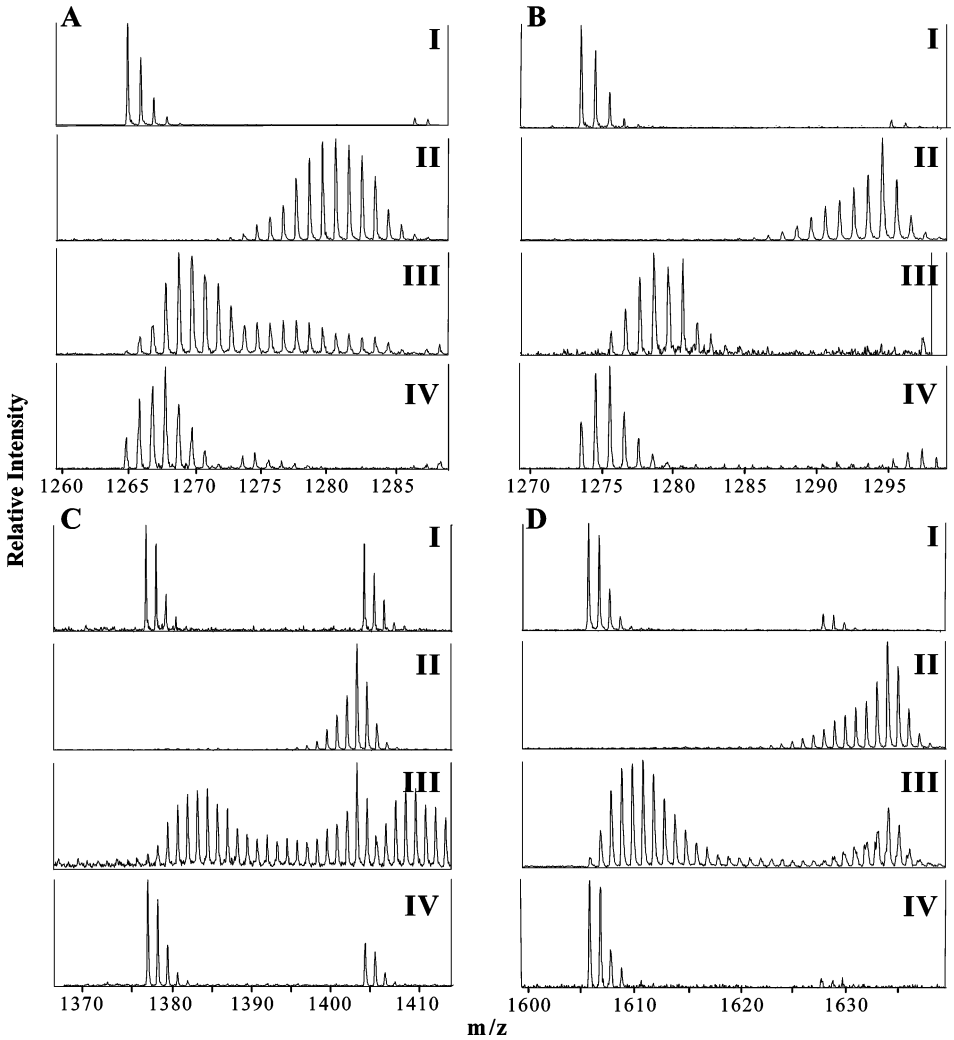

Figure 7. H/D exchange and successive back-exchange spectra for (A) LLGNVLVVVLAR (H_O), (B) LLVVYPWTQR (H_C), (C) HGTVVLTALGGILK (M_O), and (D) VEADIAGHGQEVILR (M_C) at three time intervals in a back-exchange time course: (**II**) time = 0 (after 1 h H/D exchange), (**III**) time = 10 min, (**IV**) time = 70 min. The top spectrum in each figure is before the initial H/D exchange reaction (**I**).

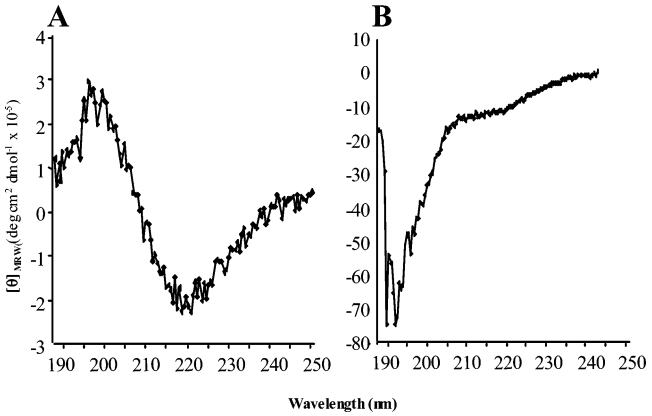

Figure 8. CD spectra for (A) LLGNVLVVVLAR (H_O) and (B) HGTVVLTALGGILK (M_O) at pH < 2.

M_O, assigned as helical in the gas-phase, exhibits strong β-hairpin character in 50:50 methanol/water (minima at 220 nm). When the water content is increased, this β-hairpin structure is apparently disrupted in favor of a random coil type conformation, possibly in combination with some small percentage of peptides (either in terms of population or regions of the molecule) adopting a helical conformation. The CD spectrum of M_O in TFE is similar to the 5:95 methanol/water solution composition, but the primary minima seems to be red-shifted approximately 2−3 nm. This observation, in combination with the appearance of a second low-intensity minimum at ∼222 nm, indicates an increase in helicity in TFE. CD data for M_C indicate helical structure in TFE that diminishes significantly (but not completely) in both methanolic solutions. Similar to H_O, CD data in TFE indicate that M_O adopts a partially helical conformation in an environment that favors intramolecular hydrogen bonding rather than intermolecular, solvent-based, hydrogen bonding, which supports gas-phase results. However, CD data in TFE for M_C are also indicative of a helical conformation. Both gas-phase ion mobility data and molecular dynamics simulations suggest that this peptide is not helical in the gas phase, which may indicate that ionic charge stabilization for this peptide sequence disrupts helix formation. In M_C charge solvation through interaction with nearby acidic residues in the peptide (specifically glu) is potentially more favorable than helix formation, which is a feature unique to M_C of the peptides considered in this study. The molecular dynamics simulations for M_C support this hypothesis (see previous section).

Peptide Conformation within the MALDI Matrix. H/D exchange mass spectrometry (Figure 7) indicates that H_O retains some hydrogen-bonded structure in the MALDI matrix, as it exhibits a broader, slower back-exchange than the control peptide (H_C). The most probable conformation for H_O within the matrix deposition is that of a β-hairpin, the same conforma-

SCHEME 1: Folding Timeline For LLGNVLVVVLAR (H_O)

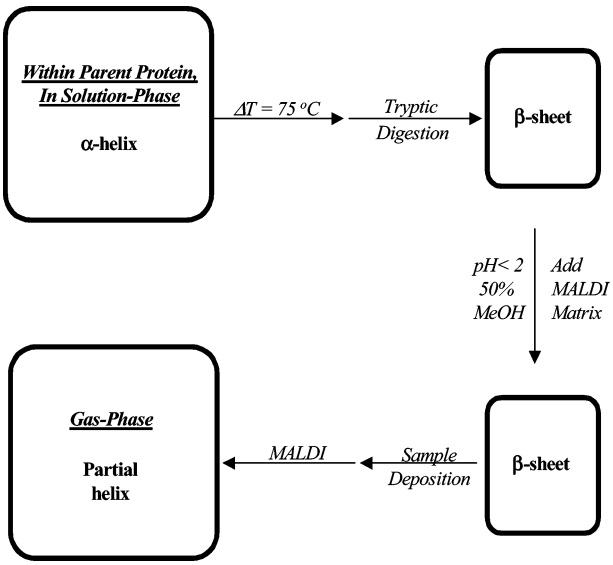

SCHEME 2: Folding Timeline For HGTVVLTALGGILK (M_O)

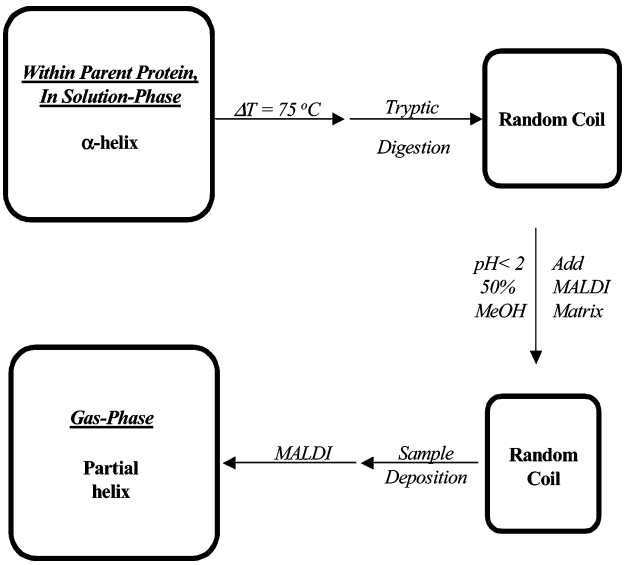

tion of the peptide in 50/50 methanol/water at pH <2. On the other hand, a helical conformation cannot be completely ruled out due to the increased packing forces present in the solidified matrix deposit. Results from solid-state NMR indicate that solution-phase conformation can be deposited into a solid environment, although a mixture of different structures can result upon mechanical denaturation.[58] Such data form the basis of the above rationale, implicating the β-hairpin conformation as the most likely major constituent of the hydrogen-bonded structure observed in Figure 7A. No clear distinction can be drawn between M_C and M_O from the H/D exchange data shown in Figure 7C,D, indicating that the outlier peptide from myoglobin is denatured (random coil) upon preparation of the sample for MALDI analysis.

Conclusions

The current literature points to a defined philosophy for interpretation of gas-phase biomolecular conformation in which the relationship between gas and solution-phase results are tenuous. Although no clear solution-phase "memory effects" (defined as the influence of starting solution-phase peptide or protein conformation on the resulting gas-phase conformation)[26] are observed, the data reported here illustrate that the conformation of gas-phase molecules is often correlated to their conformation in solution-phase environments where intramolecular hydrogen bonding is promoted (i.e., TFE). This result is, in some respects, surprising because current theories of gas-phase peptide/protein folding point to stabilization of ionic charge as the primary driving force for determining a gas-phase conformation, an effect that should be less pronounced in a solvent such as TFE.

These studies reveal two pairs of tryptic peptides with similar structural relationships, which exhibit subtle differences in terms of structural transitions upon introduction to different environments. Scheme 1 shows the progression of H_O in terms of conformation from its native structure within the β−subunit of bovine hemoglobin to the gas phase, whereas Scheme 2 illustrates a slightly different conformational progression for M_O. The summaries presented in Schemes 1 and 2 illustrate the lack of absolute structural "memory effects" for these peptide systems; i.e., the peptides exhibit different conformations dependent upon their environment (i.e., solvent dielectric, intramolecular hydrogen bonding, and proton bridging interactions) but do indicate that some peptides (i.e., H_O) can exhibit extended hydrogen-bonded structures in multiple environments. This observation is consistent with hierarchical theories of protein folding where certain protein segments are predisposed to a certain secondary structure or, as in the case observed here, exhibit a more general propensity to form highly ordered conformations. It is important to note that different MALDI sample preparations do not result in different gas-phase conformations for these peptides. In continuing research, we plan to further test the idea that a peptide or protein structure can be "trapped" as an inclusion complex in the MALDI crystal lattice and maintain a memory of this structure through the desorption and ionization process.[50,59]

The data presented here demonstrate the potential complexity of solution "memory effects" as probed (primarily) by measurements of the ion−neutral collision cross-section.[26] The solution-phase results illustrate how preparation steps for gas-phase analysis can provide peptides or proteins in a myriad of conformations prior to desorption/ionization. In addition, the gas-phase results demonstrate the difficulty of assigning secondary/tertiary structure differences in large systems, as the measured collision cross-sections correspond to a number of conformationally disparate, low-energy trial structures (i.e., β-hairpin and α-helix). In the cases reported here, the situation is made tractable by both the low absolute number of reasonable structures for the peptide ions considered here, and (more importantly) the hypothesis-driven experiments (i.e., N-terminal acetylation, sodium adduction in the case of H_O and M_O) that can rule out potential conformations. Such hypothesis driven experiments, including CD measurements in low-dielectric solvents, are of paramount importance and should be emphasized above computational results, which should be utilized only to guide further experimentation, for the determination of gas-phase conformation.

Acknowledgment. We thank Kent J. Gillig (LBMS, TAMU), Holly Sawyer (LBMS, TAMU), John A. McLean (LBMS, TAMU), Lisa M. Peréz (Laboratory for Molecular Simulation, TAMU), J. Martin Scholtz (Medicinal Biochemistry, TAMU), Jason Shcmittschmitt (Medicinal Biochemistry, TAMU), C. Nick Pace (Medicinal Biochemistry, TAMU), Jerry Tsai (Bio-

chemistry/Biophysics, TAMU), Tom Egan (Ionwerks Inc.), and Michael V. Ugarov (Ionwerks Inc.) for helpful comments and contributions. Ion mobility-mass spectrometry research at TAMU is supported by the National Science Foundation (CHE-9629966), the National Institutes of Health (1R01 RR01958701), the Department of Energy Division of Chemical Sciences, BES (DE-FG03-95ER14505), and the Texas Advance Research Program/Advanced Technology Program (TARP/TDT, 010366-0064-2001).

References and Notes

(1) Venkatraman, J.; Shankaramma, S. C.; Balaram, P. *Chem. Rev.* **2001**, *101*, 3131−3152.

(2) Dill, K. A.; Bromberg, S.; Yue, K.; Fiebig, K. M.; Yee, D. P.; Thomas, P. D.; Chan, H. S. *Protein Sci.* **1995**, *4*, 561−602.

(3) Lyubovitsky, J. G.; Gray, H. B.; Winkler, J. R. *J. Am. Chem. Soc.* **2002**, *124*, 5481−5485.

(4) Baldwin, R. L.; Rose, G. D. *Trends Biochem. Sci.* **1999**, *24*, 26−33.

(5) Shin, H. C.; Merutka, G.; Waltho, J. P.; Tennant, L. L.; Dyson, H. J.; Wright, P. E. *Biochemistry* **1993**, *32*, 6356.

(6) Bierzynski, A.; Kim, P. S.; Baldwin, R. L. *Proc. Natl. Acad. Sci. U.S.A.* **1982**, *79*, 2470.

(7) Bystroff, C.; Baker, D. *J. Mol. Biol.* **1998**, *281*, 565.

(8) Neidigh, J. W.; Fesinmeyer, R. M.; Andersen, N. H. *Nature Struct. Biol.* **2002**, *9*, 425.

(9) Robinson, C. V. *Front. Mol. Biol.* **2000**, *32*, 105.

(10) (a) Apuy, J. L.; Park, Z. Y.; Swartz, P. D.; Dangott, L. J.; Russell, D. H.; Baldwin, T. O. *Biochemistry* **2001**, *40*, 15153. (b) Apuy, J. L.; Chen, X.; Russell, D. H.; Baldwin, T. O.; Giedroc, D. P. *Biochemistry* **2001**, *40*, 15164.

(11) Powell, K. D.; Fitzgerald, M. C. *Anal. Chem.* **2001**, *73*, 3300.

(12) Powell, K. D.; Wales, T. E.; Fitzgerald, M. C. *Protein Sci.* **2002**, *11*, 841.

(13) Powell, K. D.; Ghaemmaghami, S.; Wang, M. Z.; Ma, L.; Oas, T. G.; Fitzgerald, M. C. *J. Am. Chem. Soc.* **2002**, *124*, 10256.

(14) Engen, J. R.; Smith, D. L. *Anal. Chem.* **2001**, *73*, 256A.

(15) Kim, M. Y.; Maier, C. S.; Reed, D. J.; Deinzer, M. L. *J. Am. Chem Soc.* **2001**, *123*, 9860.

(16) Demmers, J. A. A.; Rijkers, D. T. S.; Haverkamp, J.; Killian, J. A.; Heck A. J. R. *J. Am. Chem. Soc.* **2002**, *124*, 11191.

(17) (a) Campbell, S.; Rodgers, M. T.; Marzluff, E. M.; Beauchamp, J. L. *J. Am. Chem. Soc.* **1994**, *116*, 9765. (b) Gard, E.; Green, M. K.; Bregar, J.; Lebrilla, C. B. *J. Am. Soc. Mass Spectrom.* **1994**, *5*, 623. (c) Wyttenbach, T.; Bowers, M. T. *J. Am. Soc. Mass Spectrom.* **1999**, *10*, 9.

(18) (a) He, F.; Marshall, A. G.; Freitas, M. A. *J. Phys. Chem. B* **2001**, *105*, 2244. (b) Solouki, T.; Fort, R. C.; Alomary, A.; Fattahi, A. J. *Am. Soc. Mass Spectrom*. **2001**, *12*, 1272. (c) Wang, J.; Cassady, C. J. *Int. J. Mass Spectrom.* **1999**, *182/183*, 233. (d) Freitas, M. A.; Marshall, A. G. *Int. J. Mass Spectrom.* **1999**, *182/183*, 221.

(19) (a) Zhan, D.; Fenn, J. B. *Int. J. Mass Spectrom.* **2002**, *219*, 1. (b) Lee, S. W.; Freivogel, P.; Schindler, T.; Beauchamp, J. L. *J. Am. Chem. Soc.* **1998**, *120*, 11758. (c) Rodriguez-Cruz, S. E.; Klassen, J. S.; Williams, E. R. *J. Am. Soc. Mass Spectrom.* **1999**, *10*, 958.

(20) Kohtani, M.; Jarrold, M. F. *J. Am. Chem. Soc.* **2002**, *124*, 11148.

(21) (a) Kinnear, B. S.; Hartings, M. R.; Jarrold, M. F. *J. Am. Chem. Soc.* **2001**, *123*, 5660. (b) Kinnear, B. S.; Hartings, M. R.; Jarrold, M. F. *J. Am. Chem. Soc.* **2002**, *124*, 4422.

(22) Counterman, A. E.; Clemmer, D. E. *J. Phys. Chem. B* **2002**, *106*, 12045.

(23) (a) Valentine, S. J.; Anderson, J. G.; Ellington, A. D.; Clemmer, D. E. *J. Phys. Chem. B* **1997**, *101*, 3891. (b) Shelimov, K. B.; Jarrold, M. F. J. *Am. Chem. Soc.* **1997**, *119*, 2987.

(24) Badman, E. R.; Hoaglund-Hyzer, C. S.; Clemmer, D. E. *Anal. Chem.* **2001**, *73*, 6000.

(25) Arteca, G. A.; Reimann, C. T.; Tapia, O. *Mass Spectrom. Rev.* **2002**, *20*, 402.

(26) (a) Li, J.; Taraszka, J. A.; Counterman, A. E.; Clemmer, D. E. *Int. J. Mass Spectrom.* **1999**, *185/186/187*, 37. (b) Hudgins, R. R.; Woenckhaus, J.; Jarrold, M. *Int. J. Mass Spectrom. Ion Processes* **1997**, *165/166*, 497. (c) Wang, F.; Freitas, M. A.; Marshall, A. G.; Sykes, B. D. *Int. J. Mass Spectrom.* **1999**, *192*, 319.

(27) Ruotolo, B. T.; Verbeck, G. F.; Thomson, L. M.; Gillig, K. J.; Russell, D. H. *J. Am. Chem. Soc.* **2002**, *124*, 4214.

(28) Ruotolo, B. T.; Gillig, K. J.; Stone, E. G.; Russell, D. H.; Fuhrer, K.; Gonin, M.; Schultz, J. A. *Int. J. Mass Spectrom.* **2002**, *219*, 253.

(29) Park, Z. Y.; Russell, D. H. *Anal. Chem.* **2000**, *72*, 2667.

(30) Hermanson, G. T. *Bioconjugate Techniques*; Academic Press: San Diego, CA, 1996; p 785.

(31) Gillig, K. J.; Ruotolo, B. T.; Verbeck, G. F.; Stone, E. G.; Russell, D. H., submitted to *Int. J. Mass Spectrom*.

(32) McLean, J. A.; Russell, D. H. *J. Proteome Res.* **2003**, *2*, 428−431.

(33) Gillig, K. J.; Sun, W.; Russell, D. H., submitted to *Int. J. Mass Spectrom*.

(34) Fuhrer, K.; Gonin, M.; Gillig, K. J.; Egan, T.; McCully, M. I.; Schultz, J A. *PCT Int. Appl.* **2002**, WO 0297383, 35 pp.

(35) Ruotolo, B. T.; Gillig, K. J.; Stone, E. G.; Russell, D. H. *J. Chromatogr. B* **2002**, *782*, 385.

(36) Valentine, S. J.; Counterman, A. E.; Clemmer, D. E. *J. Am. Soc. Mass Spectrom*. **1999**, *10*, 1188.

(37) Shoff, D. B.; Harden, C. S. *Int. Workshop Ion Mobility Spectrom., 4th* **1995**.

(38) Wyttenbach, T.; von Helden, G.; Bowers, M. T. *J. Am. Chem. Soc*. **1996**, *118*, 8355.

(39) http://www.indiana.edu/∼clemmer/.

(40) Voet, D..; Voet, J. G. *Biochemistry*, 2nd ed.; John Wiley and Sons: New York, NY, 1995; p 1361.

(41) http://webbook.nist.gov/chemistry/.

(42) (a) Hudgins, R. R.; Mao, Y.; Ratner, M. A.; Jarrold, M. F. *Biophys. J*. **1999**, *76*, 1591. (b) Hudgins, R. R.; Ratner, M. A.; Jarrold, M. F. *J. Am. Chem. Soc.* **1998**, *120*, 12974−12975.

(43) http://nano.chem.indiana.edu/software.html.

(44) Mesleh, M. F.; Hunter, J. M.; Shvartsburg, A. A.; Schatz, G. C.; Jarrold, M. F. *J. Phys. Chem.* **1996**, *100*, 16082.

(45) Shvartsburg, A. A.; Siu, K. W. M.; Clemmer, D. E. *J. Am. Soc. Mass Spectrom*. **2001**, *12*, 885.

(46) Scaled intrinsic size parameters have been reported to predict collision cross-section of random coil peptides to ca. 1% average RSD.

(47) Dugourd, Ph.; Hudgins, R. R.; Clemmer, D. E.; Jarrold, M. F. *Rev. Sci. Instrum*. **1997**, *68*, 1122.

(48) Wolynes, P. *Proc. Natl. Acad. Sci. U.S.A.* **1995**, *92*, 2426.

(49) Jarrold, M. F. *Annu. Rev. Phys. Chem.* **2000**, *51*, 179.

(50) Tzakos, A. G.; Bonvin, A. M. J. J.; Troganis, A.; Cordopatis, P.; Amzel, M. L.; Gerothanassis, I. P.; van Nuland, N. A. J. *Eur. J. Biochem.* **2003**, *270*, 849.

(51) Abagyan, R.; Argos, P. *J. Mol. Biol*. **1992**, *225*, 519.

(52) Kinnear, B. S.; Kaleta, D. T.; Kohtani, M.; Hudgins, R. R.; Jarrold, M. F. *J. Am. Chem. Soc.* **2000**, *122*, 9243.

(53) Li, A.; Fenselau, C.; Kaltashov, I. A. *Proteins: Struct. Funct. Genet. Suppl.* **1998**, *2*, 22.

(54) Kohtani, M.; Kinnear, B. S.; Jarrold, M. F. *J. Am. Chem. Soc.* **2000**, *122*, 12377.

(55) Ruotolo, B. T.; Tate, C. C.; Russell, D. H. *J. Am. Soc. Mass Spectrom.* **2004**, *15*, 870.

(56) (a) Buck, M. *Quarterly Rev. Biophys*. **1998**, *31*, 297. (b) Roccatano, D.; Colombo, G.; Fioroni, M.; Mark, A. E. *Proc. Natl. Acad. Sci. U.S.A.* **2002**, *99*, 12179.

(57) Dwyer, D. S. *Biopolymers* **1999**, *49*, 635.

(58) Henzler Wildman, K. A.; Lee, D.-K.; Ramamoorthy, A. *Biopolymers* **2002**, *64*, 246.

(59) Sawyer, H. A.; Marini, J. T.; Stone, E. G.; Ruotolo, B. T.; Gillig, K. J.; Russell, D. H., submitted to *J. Am. Soc. Mass Spectrom*.